53. Understanding of the formation mechanism of sea fog through numerical simulation using a Single Column Model coupled with WRF

Chang Ki Kim* and Seong Soo Yum
Department of Atmospheric Sciences, Yonsei University, Seoul 120-749, Korea

1. Introduction

Fog is a meteorological phenomenon that can be a great hazard in the airport. Incheon International Airport (hereafter IIA) is located on a partly reclaimed island on the west of coast of Korea so that IIA often suffers from visibility degradation due to sea fogs. The number of sea fogs occurred over the IIA area is 35 from 2002 to 2006. However, a clear guidance to forecast the sea fog is not made yet since the formation and dissipation of sea fog are complicated. Therefore in order to accomplish a clear guidance, physical mechanism for the formation and dissipation of sea fog should be primarily understood.

Kim and Yum (2010) examined the statistical characteristics of the sea fog that forms over the Yellow Sea off the west coast of Korea. They classified 35 sea fogs into 26 cases of cold sea fog and 9 cases of warm sea fog, based on the differences between T and sea surface temperature (SST) (TSST = T – SST) 3 h before the onset time of fog formation (i.e., cold sea fog for TSST > 0 and warm sea fog for TSST < 0) and linked the occurrence statistics with relevant meteorological variables. As an effort to further this finding, Kim and Yum (2011) identified the relative contributions of turbulence, advection and radiation on T and T_d in the atmospheric boundary layer over the Yellow Sea. They found that the decrease of T due to turbulence over colder sea surface and radiative cooling could result in water vapor saturation in the stable boundary layer to form a cold sea fog; however, warm sea fog was formed by increasing the amount of water vapor within the convective boundary layer due to turbulent mixing of water vapor over the warm sea surface.

The purposes of this study are twofold. The first is to analyze the meteorological properties related to the formation and dissipation of the classified fogs through numerical modeling. The second is to study the feasibility for the operation prediction. The numerical simulations using the 3D operation model with a very high horizontal and vertical resolution requires too expensive computation cost. Recently, 1D turbulence model with a very high vertical resolution coupled with a 3D regional model is used to reduce the computation cost to predict the fog occurrence within PBL.

2. Case Description

T, SST, T_d, relative humidity (RH), wind

* *Corresponding Author Address*: Chang Ki Kim, Cloud Physics Laboratory, Department of atmospheric Sciences, College of Science, Yonsei University, Seoul, Korea
E-mail: 62beatle@yonsei.ac.kr

direction (WD), wind speed (WS) and mean sea level pressure (SLP) are measured every hour at a buoy near Dukjeok Island, 40 km from Incheon International Airport (hereafter IIA, Fig. 1). Rawinsonde is launched from the weather station at Baeknyeong Island every day at 00 UTC (09 local standard time, LST) and 12 UTC (21 LST).

This study selected the 18 April 2006 case among the 26 cold sea fog cases classified by Kim and Yum (2010). Figure 2 shows the time variation of the T, SST, T_d and RH measured at the buoy during this episode of cold sea fog, observed from 19 UTC, 18 April to 05 UTC, 19 April, based on the 95% RH criterion. The T gradually decreases from 00 to 17 UTC, 18 April and then it decreases fast to the onset time of sea fog (19 UTC, 18 April) with -0.8 $^{o}C\ h^{-1}$. Strong cooling rate during this period may be due to nocturnal radiative cooling that enhances the turbulent cooling induced by positively large TSST. Meanwhile, the T_d rapidly increases from 00 to 03 UTC, 18 April and then it gradually increases with fluctuation. The TSST was the lowest at 02 UTC, 19 April due to the decrease of T during the fog. Radiative cooling plays a role in decreasing T at the fog top.

In addition to the radiative effect, cold advection may contribute to the decrease of T. The T_d decreased as the saturation vapor pressure decreased with T decrease in the mature phase of the sea fog once water vapor saturation is attained. In the dissipation phase, T remained constant, but T_d was reduced.

3. Model Description

In this study, WRFV3.1.1 is used as a 3D regional model and PArameterized FOG (PAFOG) model is employed as a 1D, single column turbulence model. Since WRF is world wide common model, PAFOG will be described here. PAFOG is developed by the University of Bonn, Germany (Bott and Trautmann, 2002). PAFOG is designed for studying stable boundary layer as well as convective boundary layer with Mellor-Yamada 2.5 level turbulence closure and also supports sophisticated double moment scheme for the cloud species.

4. Numerical Experimental Design

4.1 WRF

Numerical simulation is performed for 3 domains with one-way grid nesting procedure. Domain 3 with the finest horizontal resolution of 2 km, which is centered on IIA, resolves the evolution of sea fog, as well as the local meteorological characteristics off the west coast of the Korean Peninsula. Table 1 summarizes the model configuration of WRF.

4.2 PAFOG

In this study, the vertical resolution of the model is set to be high so that the model equations are solved at 400 levels distributed between the surface and the altitude of 2500 m, using a constant resolution of 5 m for grids from the surface to 1500 m and a logarithmic spacing from 1500 m to the top

of the model. A total of ten additional levels from 2500 m to the top of the atmosphere are used only for radiative transfer equations. The integration time interval is 5 s.

4.3 Coupling of PAFOG with WRF

This study uses two approaches to couple between PAFOG and WRFV, i.e., Eulerian approach and Lagrangian approach. In the Eulerian approach, hourly horizontal advections of heat and moisture produced by WRF are added hourly into the tendency equations of T and Td of PAFOG as an external forcing. This study prescribes that the single column of PAFOG is located at the buoy near Dukjeok Island.

The θ and T_d at the grid corresponding to the buoy location from the WRF output are used as the initial profiles for the Eulerian approach. SST is held constant in this approach since observed SST in Fig. 2 is nearly constant. The vertical profile of θ in Fig. 3a represents the typical characteristics of a stable boundary layer. SST and wind speed at an altitude of 2.5 km were 281 K and 16.1 m s^{-1}, respectively, in the simulation executed from 00 UTC, 17 April to 12 UTC, 19 April.

Contrary to the Eulerian approach, the Lagrangian approach considers the single column moving along with the trajectory given by WRF. To perform the desired simulation using this approach, our model is modified to account for specified time-varying lower boundary conditions for heat and moisture. The initial conditions for the Lagrangian approach were the vertical profiles of θ and T_d at the starting point of the trajectory (Fig. 3b).

5. Results

5.1 Model Evaluation

Performance of PAFOG was first evaluated before the numerical simulation of the selected case. The threat score was used for the evaluation of PAFOG in the Eulerian approach. The threshold values of the threat score for the observation and simulation were 95% RH at the buoy near Dukjeok Island and a 0.005 g kg^{-1} cloud water mixing ratio at the lowest level of PAFOG, respectively.

The threat score of PAFOG for the selected case was 0.92, which was much better than that of WRF (0.51) and the mean threat score for all 26 cold sea fog cases was 0.79 for PAFOG and 0.61 for WRF simulations. Figure 4 shows the time-height plot of the cloud water mixing ratio at the buoy location from the two models. WRF tended to simulate deep fog, the depth of which is greater than 1.5 km, and incomparable to the fog depth estimated from the MTSAT-1 geostationary satellite data (Fig. 4a). On the other hand, the simulated fog depth from PAFOG was consistent with the satellite estimated fog depth, except for the maximum value (e.g., at 03 UTC 19, April in Fig. 4b). In the Lagrangian approach, the performance of PAFOG is also better than that of WRF. The sea fog formed 30 hours earlier and fog depth is much higher in

the WRF simulation than observation (Fig. 4c). In contrast to WRF, the evolution of the fog layer in the PAFOG simulation was similar to that of the satellite estimated fog layer (Fig. 4d).

5.2 Eulerian Approach

Figure 5a shows the time series of T, T_d, SST, and the integrated liquid water path (LWP) at an altitude of 5 m for the Eulerian approach. Therefore the rapid decrease of T during 3 hours after simulation began results from the spin-up effect. In the simulation, fog is formed 1 h later than observation and is dissipated 3 h later than observation. The T and T_d gradually increases 03 UTC, 17 April to 18 UTC, 18 April and then the fast decrease of T is found until the onset time of sea fog (Fig. 5a). The simulation of PAFOG captures the strong cooling prior to the onset time of sea fog in Fig. 2. Kim and Yum (2011) argued that radiative and turbulent cooling contributed to a decrease of T before the formation of sea fog. The relative contribution of turbulence, advection and radiation to the fast decrease of T will be presented in the conference.

The T_d increased slightly from 06 UTC, 17 April to the onset time of sea fog (20 UTC, 18 April) despite the turbulent moisture loss (Fig. 5a). This may imply that moisture advection as an external force compensates for the turbulent loss of water vapor

5.3 Lagrangian Approach

The air was gradually heated over the warm sea surface from 00 to 09 UTC, 17 April (Fig. 5b). T_d also increased due to the turbulent mixing of moisture over the warm sea surface. However, T did not increase, even when the sea surface is still warmer from 09 to 15 UTC, 17 April. This is due to the fact that the nocturnal radiative emission cooled the air after sunset (09 UTC; 6 PM locally). After the air column moved over the cold sea surface, water vapor saturation was attained due to the decrease of T, in spite of the decrease of T_d. The variations in T and T_d before the onset of cold sea fog can be affected by the interaction with the cold sea surface like in the Eulerian approach. Thus, the formation mechanism of cold sea fog is similar to that of typical advection fog: the air column over the warm sea surface moved over the cold sea surface, and then the water vapor saturation was achieved by radiative and turbulent cooling over the cold sea surface.

Once fog has been formed, the contributions of radiation and turbulence to the development of the fog layer increase. The results from the numerical simulation in our study support the presence of radiative cooling at the fog top and its effect on the vertical growth of the fog layer. These also presented in the conference

6 Conclusion

We simulated the influences of turbulence, advection and radiation on the formation of sea fog over a cold sea surface near the west coast of the Korean Peninsula

using a 1D turbulence model, PAFOG, coupled with a 3D regional model, WRF. This study uses an Eulerian approach and a Lagrangian approach to couple the PAFOG with WRF. In the Eulerian approach, horizontal advections of heat and moisture, produced every hour with the WRF, are provided as external forcings into PAFOG. Conversely, the Lagrangian approach considers a single column moving with a trajectory given by WRF. The predictability of PAFOG coupled with WRF is greater than that of WRF alone, as WRF tends to overestimate the depth of the fog layer. The decrease in air temperature associated with sea fog is governed by turbulence and radiation. Radiative cooling elevates the top of the fog cloud, which destabilizes the entire fog layer.

Acknowledgement

This work was funded by the Korea Meteorological Administration Research and Development Program under Grant RACS_2010-5001.

References

Bott, A., and T. Trautmann, 2002: PAFOG--a new efficient forecast model of radiation fog and low-level stratiform clouds. *Atmos. Res.*, **64,** 191-203.

Kim, C. K., and S. S. Yum, 2010: Local meteorological and synoptic characteristics of fogs formed over Incheon international airport in the west coast of Korea. *Adv. in Atmos. Sci.*, **27,** 761-776.

——, 2011: Marine Boundary Layer Structure for the Sea Fog Formation off the West Coast of the Korean Peninsula. *Pure Appl. Geophys.*, Published in internet based journal.

Table 1. Summary of the WRF simulation conditions

	Domain 1	Domain 2	Domain 3
Grid spacing	18 km	6 km	2 km
Time step	108 s	36 s	12 s
IC/BC	NCEP GDAS	1 domain	2 domains
PBL	YSU	YSU	YSU
Microphysics	WSM6	WSM6	WSM6
Convection	KF	KF	
Number of vertical layers		65	
The lowest level		0.998 (sigma-level)	
Soil model		Five-layer soil model	

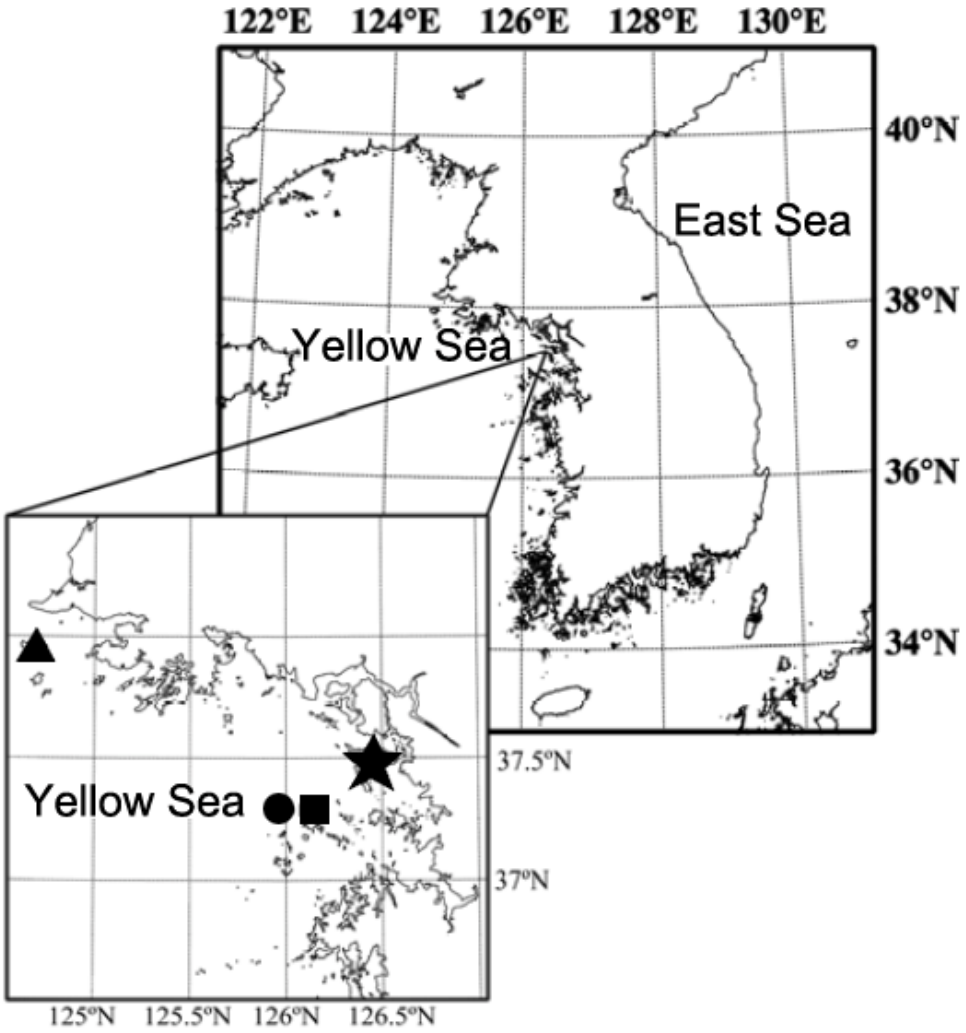

Fig. 1. The locations of Incheon International Airport (IIA) and the other measurement sites. The asterisk, the closed circle, the triangle, and the rectangle indicate IIA, the buoy located near Dukjeok Island, the radiosonde site at Baeknyeong Island, and the lighthouse at Seonmi Island, respectively.

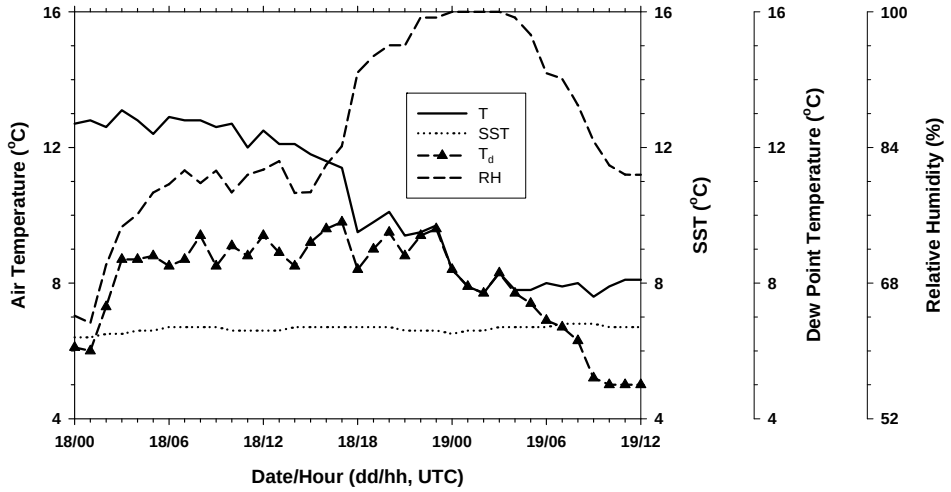

Fig. 2. Time series of air temperature (T, solid line), SST (dotted line), dew point temperature (T_d, dashed line with closed triangle) and related humidity (RH, dashed line) measured at the buoy.

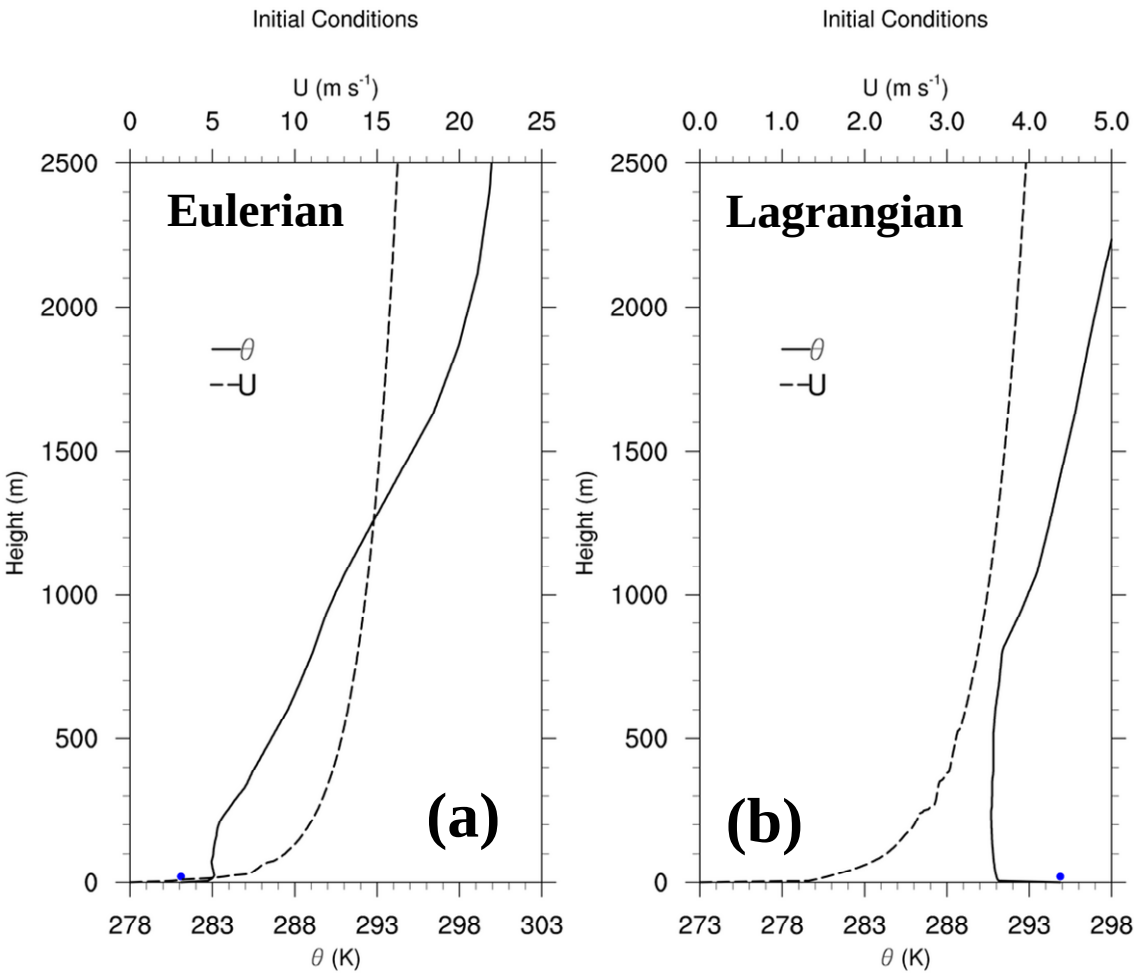

Fig. 3. Initial conditions of potential temperature (K) and zonal wind speed (m s^{-1}) for the PAFOG simulation using the Eulerian approach (a) and the Lagrangian approach (b). The dot at the surface altitude in each plot indicates the SST (K) at the initial time.

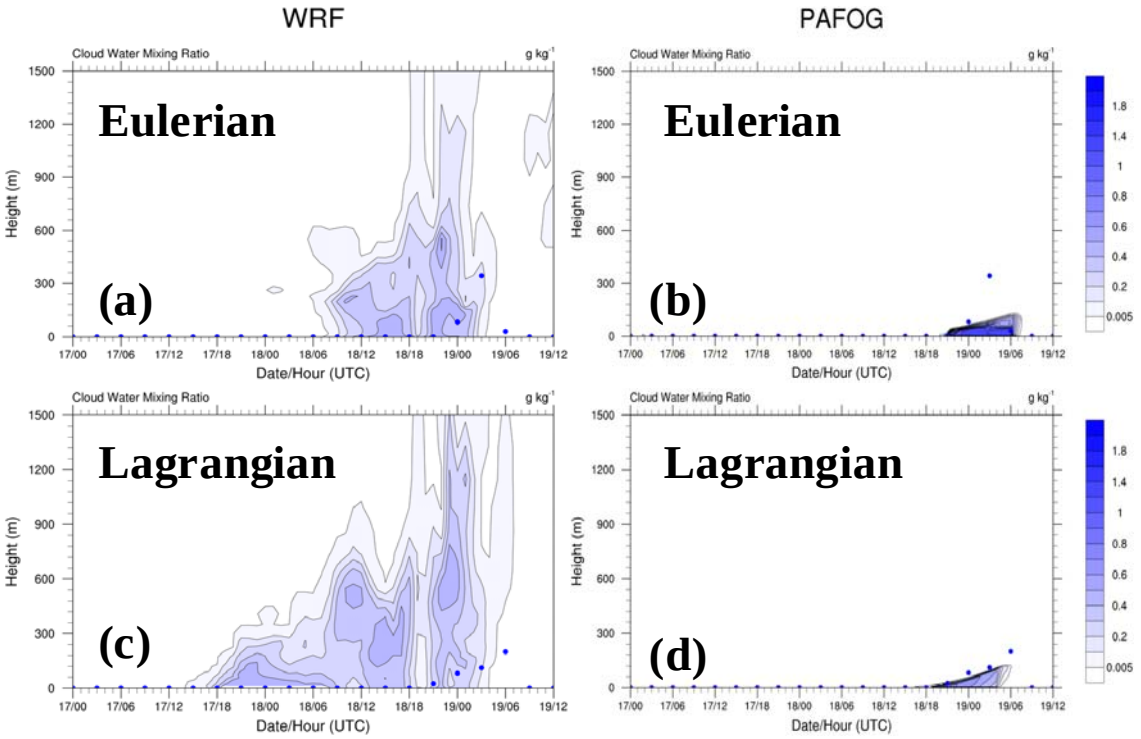

Fig. 4. Time-height plot of cloud water mixing ratio (g kg^{-1}) for WRF and PAFOG with the Eulerian approach (a, b) and with the Lagrangian approach (c, d). The dot in each plot indicates the estimated height of the fog top from the MTSAT-1 satellite.

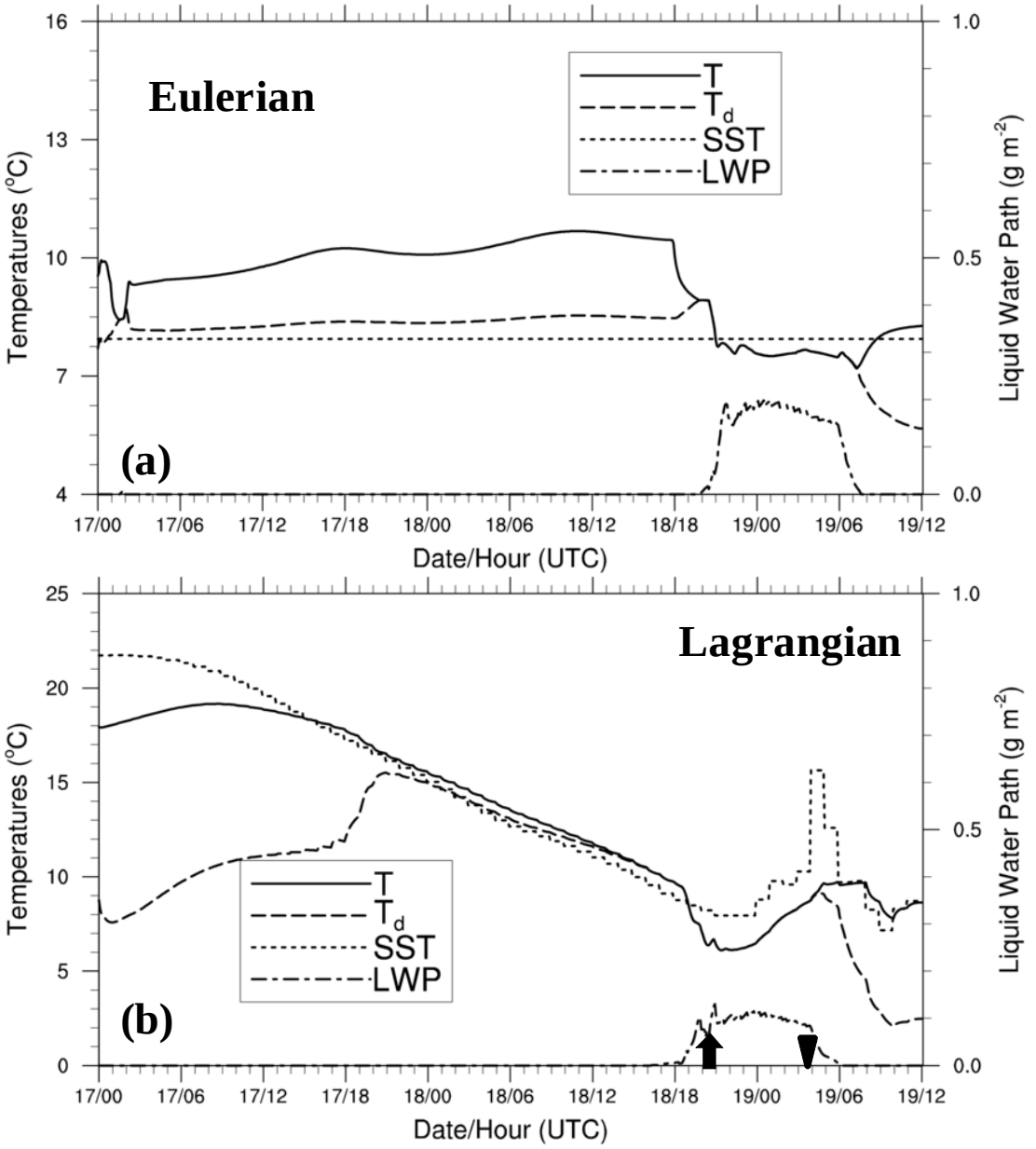

Fig. 5. Time series of T (solid line, ℃), T_d (dashed line, ℃), SST (dotted line, ℃) and liquid water path (LWP, dash-dotted line, g m^{-2}) with the Eulerian approach (a) and the Lagrangian approach (b). In (b) the arrow indicates the time that the air column is located at the buoy (arrow) and the triangle indicates the time that the air column moves onto the land.